CAN-2023-0103-ver9-Marquez_1P
Type: research-article
Cannabis and Cannabinoid Research
Volume 0, Number 0, 2023

DOI: 10.1089/can.2023.0103

Open camera or QR reader and scan code to access this article and other resources online.

ORIGINAL RESEARCH

Broad-Spectrum Antiviral Effect of Cannabidiol Against Enveloped and Nonenveloped Viruses

Agostina Marquez,[1,2] Josefina Vicente,[1,2] Eliana Castro,[3] Daiana Vota,[2,4] María Soledad Rodríguez-Varela,[5] Priscila Ailín Lanza Castronuovo,[6] Giselle Magali Fuentes,[7–9] Alejandro Parise,[6,10] Leonardo Romorini,[5] Diego Alvarez,[11] Carlos Bueno,[1,2] Cristina Ramirez,[10,12] Agustina Alaimo,[2] and Cybele García[1,2,*]

Abstract

Cannabidiol (CBD), the main nonpsychoactive cannabinoid of the *Cannabis sativa* plant, is a powerful antioxidant compound that has attracted more attention in recent years due to its effects on a variety of biological functions. Zika virus (ZIKV) is a virus transmitted mainly by the *Aedes aegypti* mosquitoes, which causes severe neurological diseases, such as microcephaly and Guillain-Barre syndrome, mainly in fetuses and newborns. Although the frequency of viral outbreaks has increased recently, no vaccinations or particular chemotherapeutic treatments are available for ZIKV infection. In this study, we report that CBD inhibits the replication of ZIKV and other arboviruses with major epidemiological significance such as dengue and chikungunya. Furthermore, we present encouraging findings that outline a potential mechanism of action for CBD's antiviral efficacy against ZIKV. We determined that CBD affects cellular membranes and, in particular, lowers intracellular cholesterol levels, thus affecting ZIKV viral replication. Finally, we demonstrate that CBD inhibits structurally dissimilar viruses, suggesting that this phytochemical has broad-spectrum antiviral effect, representing a valuable alternative in emergency situations during viral outbreaks, like the one caused by severe acute respiratory syndrome coronavirus 2 in 2019.

Keywords: cannabidiol; antiviral; Zika; cholesterol; broad spectrum

Introduction

Natural compounds have been one of the most successful sources of medicines and pharmaceutical drugs. Since 1981, chemical factors derived from herbal and plants, as well as their derivatives and mimetic compounds have represented almost two-thirds of the new small-molecule drugs.[1,2] The *Cannabis sativa* plant has more than 445 thousand chemical compounds, including cannabinoids, terpenes, and flavonoids. At least 120 of these phytochemicals have been identified as cannabinoids, of which the most abundant are cannabidiol (CBD) and Δ-9-tetrahydrocannabinol (Δ^9-THC).[3] CBD is a 21-carbon terpenophenolic compound that lacks the unwanted psychoactive effects of

[1]Laboratorio de Virología, Departamento de Química Biológica, Facultad de Ciencias Exactas y Naturales, Universidad de Buenos Aires (UBA), Buenos Aires, Argentina.
[2]Instituto de Química Biológica de la Facultad de Ciencias Exactas y Naturales (IQUIBICEN), UBA–Consejo Nacional de Investigaciones Científicas y Técnicas (CONICET), Buenos Aires, Argentina.
[3]Instituto de Investigaciones Biotecnológicas (IIBIO), Universidad Nacional de San Martín (UNSAM)–(CONICET), Buenos Aires, Argentina.
[4]Laboratorio de Inmunofarmacología, IQUIBICEN, UBA-CONICET, Buenos Aires, Argentina.
[5]Laboratorio de Investigación Aplicada a Neurociencias (LIAN), Fundación para la Lucha contra las Enfermedades Neurológicas de la Infancia (Fleni)-CONICET, Instituto de Neurociencias (INEU), Buenos Aires, Argentina.
[6]Instituto de Investigaciones en Biodiversidad y Biotecnología (INBIOTEC), Química Analítica y Modelado Molecular (QUIAMM), Universidad Nacional de Mar del Plata–CONICET, Mar del Plata, Argentina.
[7]Instituto de Investigaciones en Producción Sanidad y Ambiente (IIPROSAM), Facultad de Ciencias Exactas y Naturales, Universidad Nacional de Mar del Plata, Centro Científico Tecnológico Mar del Plata, CONICET, Mar del Plata, Argentina.
[8]Centro de Asociación Simple CIC PBA, Mar del Plata, Argentina.
[9]Centro de Investigaciones en Abejas Sociales, Facultad de Ciencias Exactas y Naturales, Universidad Nacional de Mar del Plata, Mar del Plata, Argentina.
[10]Departamento de Química Biológica y Bioquímica, Facultad de Ciencias Exactas y Naturales, Universidad Nacional de Mar del Plata, Mar del Plata, Argentina.
[11]Escuela de Bio y Nanotecnologías (EByN), Universidad Nacional de San Martín, Buenos Aires, Argentina.
[12]Asociación Civil CBG2000, Mar del Plata, Argentina.

*Address correspondence to: Cybele García, Laboratorio de Estrategias Antivirales, Instituto de Química Biológica de la Facultad de Ciencias Exactas y Naturales (IQUIBICEN), Universidad de Buenos Aires–CONICET, Ciudad Universitaria, Pab. 2, piso 4, 1428, Buenos Aires, Argentina, E-mail: cygarcia@qb.fcen.uba.ar

F1 ▶ some cannabis derivatives (Fig. 1a). This phytocannabinoid is a powerful antioxidant and anti-inflammatory compound[4] that acts on various molecular targets, being able to cause effects in a wide range of biological functions with potential beneficial applications for health care purposes.

Despite what is known so far, the search for new applications of CBD medicine continues to be an agenda in scientific matters. CBD has been extensively studied for years in the field of neuroscience.[5–7] Also, it has been reported that CBD could inhibit the proliferation of cancer cells, exerting an antitumor effect.[8–11] On the contrary, it has been suggested that this cannabinoid could have a positive impact on cardiovascular diseases such as cardiomyopathies and arterial hypertension.[12,13]

Sea et al. and Mabou Tagne et al. have carried out extensive reviews, in which several research reports proved that CBD have antiviral effects.[3,14] In this sense, CBD has been shown to be active against hepatitis C virus,[15] HIV[16,17] and against severe acute respiratory syndrome coronavirus 2 (SARS-CoV-2).[18–20] Particularly, many reports focused on SARS-CoV-2 infections and proposed that the use of CBD could be beneficial against the characteristic symptoms caused during cytokine storm.[21] Despite the efforts made in relationship to its antiviral activity, there are no reports of the effect of CBD on neglected, tropical, and vector-borne diseases. For this reason, the major aim of this study was to explore the *in vitro* antiviral activity of this small molecule against Zika virus (ZIKV).

This mosquito-borne Flavivirus has become a relevant emerging viral pathogen due to its recently expansive spread around the world.[22] To note, ZIKV infection can also be parenterally and sexually transmitted to humans, producing outbreaks sporadically associated to neurological disorders and microcephaly.[23] No vaccines or specific chemotherapy are

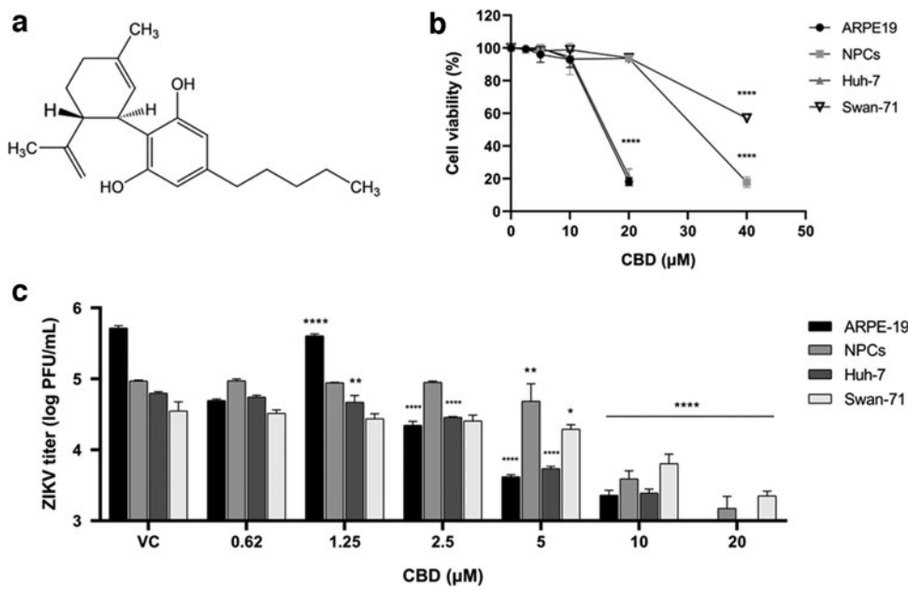

FIG. 1. Antiviral activity of CBD against ZIKV in relevant cellular targets. **(a)** Chemical structure of CBD. **(b)** Cell viability of ARPE-19, NPCs, Huh-7, and Swan-71, determined by the MTT reduction assay. **(c)** Antiviral activity of CBD against ZIKV. Cells were infected with ZIKV and treated with different concentrations of CBD (0.6–10 μM) during 48 h; 20 μM CBD was also evaluated in NPCs and Swan-71 cells. After that, supernatants were harvested and titrated by the plaque assay. Viral control (VC): untreated infected cells. Data are presented as mean ± SD ($n = 3$). ANOVA followed by Dunnett's *post hoc* analysis was used to calculate the *p*-values. ****$p < 0.0001$, **$p < 0.01$, *$p < 0.05$ versus control. ANOVA, analysis of variance; CBD, cannabidiol; MTT, 3-(4,5-dimethylthiazol-2-yl)-2,5-diphenyl tetrazolium bromide; NPCs, neural progenitor cells; ZIKV, Zika virus.

currently available for ZIKV infection, denoting the need of effective antiviral agents. Here, we show promising results describing the possible mechanism of actions involved in CBD antiviral activity against ZIKV and other nonrelated viruses, suggesting that this phytochemical has broad-spectrum antiviral effect, representing a valuable alternative for the treatment of viral diseases.

Materials and Methods

Cannabidiol extraction and purification

Fifty grams of inflorescences finely chopped and previously decarboxylated at 120 degrees for 40 min were suspended in ethanol with vigorous stirring for 30 min. This process was carried out three times on the starting material. Next, it was dried using a rotary evaporator, and the extract was purified by means of column chromatography, using silica gel (Merck 60; 0,015-0,040). The solvent gradient used was hexane:ethyl acetate from 90:10 to 30:70. This process was repeated twice to achieve maximum purification.

The characterization of the product was carried out AU7 ▶ by means of HPLC as follows: The quantitative analysis of CBD was performed to determine purity using a chromatograph provided of a UV-Visible photodiode array detector (UV2000-Thermo Separation Products) equipped with a reverse-phase Zorbax SB-Aq column 4.6 mm ID × 250 mm, 5 μm. A mixture of (85:15) methanol and ultrapure water with a flow rate of 1 mL/min was used as eluent and the detection was performed at $\lambda = 220$ nm.[24] The concentration of CBD in the dilution was determined using the external standards calibration curve method and the retention time was used as an identification criterion. The struc- AU8 ▶ ture was also confirmed using CG-MS, comparing with the Wiley and NIST libraries. Purity was 99.8%. For experimental assays, a 10 mM CBD stock was prepared by dissolving the phytochemical in absolute ethanol of analytical grade.

Cells and viruses

Vero (African green monkey kidney) (ATCC®; CCL-81), Huh-7 (human liver carcinoma) (ATCC; CRL-8024), A549 (human lung adenocarcinoma) (ATCC; CCL-185™), and ARPE-19 (human retinal pigment epithelium) (ATCC; CRL-2302TM) cell lines were grown in Eagle's minimal essential medium (MEM; Gibco, Carlsbad, CA, USA) supplemented with 5% heat-inactivated fetal bovine serum (FBS) and 50 μg/mL gentamicin. First-trimester trophoblast cell line (Swan-71) was grown in Dulbecco's modified Eagle's medium and Nutrient Mixture F12 (DMEM-F12) supplemented with 10% FBS, 2 mM glutamine, and 100 U/mL streptomycin–100 μg/mL penicillin solution.

Human neural progenitor cells (NPCs) were derived from H9 human embryonic stem cells (WiCell Research Institute) by using a commercial kit from ThermoFisher Scientific (PSC Neural Induction Medium; Gibco) and maintained in DMEM-F12 supplemented with B27 1X, N2 1X, 2 mM glutamine, 2 mM nonessential amino acids, 100 U/mL streptomycin–100 μg/mL penicillin solution, 20 ng/mL epidermal growth factor (EGF), and 20 ng/mL basic fibroblast growth factor (bFGF).

The following viruses were used: ZIKV, Argentine strain INEVH116141; dengue virus, serotype 2 (DENV-2), strain Thailand/16681/1984; yellow fever virus (YFV), strain 17D; chikungunya virus expressing ZsGreen fluorescent protein (CHIKV-ZsGreen) obtained following transfection of BHK cells with the genomic RNA synthesized *in vitro* using the infectious cDNA clone of the virus expressing ZsGreen as a template, as previously described[25]; Junín virus (JUNV), strain IV4454; herpes simplex type 1 (HSV-1), strain F; adenovirus type 5 (ADV-5); and poliovirus type 1 (PV-1).

Cell viability assay

Cell cultures grown in 96-well plates were exposed for 72 h at a concentration range of 2.5 to 20 μM (two-fold dilutions, three wells per concentration) of CBD. Particularly, in Swan-71 cells and NPCs, concentrations of 2.5 to 40 μM were tested. Viability was determined by 3-(4,5-dimethylthiazol-2-yl)-2,5-diphenyl tetrazolium bromide (MTT; Sigma-Aldrich Co., St. Louis, MO, USA) method. For this, after 72 h of exposure to the compound, the medium was removed and 100 μL of medium containing MTT (0.5 mg/mL) were added. The plate was incubated for 1 h at room temperature and then the formed formazan crystals were dissolved in 100 μL of ethanol, 96% v/v. Absorbance was measured at 570 nm on a POLARstar Omega microtiter plate reader (BMG LABTECH, Ortenberg, Germany).

Viral infections and treatments

Cells grown in 96-well plates were infected with a multiplicity of infection (MOI) of 0.1 for ZIKV, DENV, YFV, JUNV, ADV-5, and 0.07 for HSV-1 and PV-1. In particular, Swan-71 cells were infected with ZIKV

at MOI = 1. After 1 h of incubation at 37°C, the inocula were removed and fresh medium was added. For treatments, CBD stock was diluted in medium to final concentrations in the range of 0.6–10 μM. MEM supplemented with 1.5% FBS was used for Vero, Huh-7, and A549 cells; DMEM-F12 supplemented with 10% FBS was used for Swan-71 cells; DMEM-F12 supplemented with B27 1X, N2 1X, EGF (20 ng/mL), and bFGF (20 ng/mL) for NPCs. Solutions were added to infected cells and incubated at 37°C for 24 h for PV-1 and 48 h for the other viruses (three wells per concentration).

After incubation, the supernatants were harvested and titrated by the plaque assay. All the works were performed under strict level 2 biosafety working conditions. Protocols involving infectious agents were approved by the Office of Environmental Health and Safety at the School of Sciences of the University of Buenos Aires.

Plaque assay

Vero and A549 (for ADV-5) cells were seeded into 24-well microplates and grown overnight. Ten-fold dilutions of the sample were added to cell monolayers and then were incubated at 37°C for 1 h. After incubation, the inoculum was removed and monolayers were covered with MEM that contained 1% methylcellulose. Cells were incubated at 37°C for 24 h (for PV-1), 72 h (for ZIKV and HSV-1), 5 days (for ADV-5 and YFV), and 7 days (for DENV-2 and JUNV). Finally, plaques were fixed with 10% formaldehyde and stained with 1% crystal violet in 10% ethanol and counted. The virus titer was expressed as plaque-forming units per milliliter.

Focus-forming assay

The assay was carried out in Vero cells grown in 96-well plates. Cells were infected with the reporter virus CHIKV-ZsGreen[25] (MOI = 0.02) and CBD solutions with different concentrations (1.25–10 μM) were added. Treated cells were incubated for 20 h at 37°C in an incubator with 5% CO_2. Subsequently, the supernatants were discarded, and cells washed with PBS and fixed with 4% paraformaldehyde (PFA) for 1 h at 4°C. Afterward, PBS washes were carried out once again and 30 μL of PBS were added. Finally, the count of fluorescent foci was carried out in an ELISpot equipment and InmunoSpot 7.0.30.2 software (ImmunoSpot C.T.L, Germany).

Measurement of interleukin-6 and interleukin-8 by enzyme-linked immunosorbent assay

Interleukin-6 (IL-6) and interleukin-8 (IL-8) were determined by the enzyme-linked immunosorbent assay (ELISA). For this, Huh-7 cells were infected with the ZIKV (MOI = 0.1) and subsequently treated for 48 h with a 10 μM CBD concentration. These ILs were also determined in Huh-7-uninfected cells. Cytokines measurements were performed on cell culture supernatants using the BD OptEIA™ ELISA sets (Becton Dickinson) following the manufacturer's instructions.

Time-of-drug addition assay

Vero and Huh-7 cells were grown in 24-well microplates overnight. Cells were infected with ZIKV (t = 0 h; MOI = 0.5) in the presence or absence of 10 μM CBD at 4°C. After 2 h, cells were washed three times with PBS and fresh medium was added. CBD of 10 μM was added at 0, 2, 4, 6, and 8 h postinfection (hpi). Supernatant were collected at 24 hpi and titrated by plaque assay.

Viral inactivation assay

ZIKV was exposed to 5 and 10 μM CBD for 1.30 h at 37°C. Control group consisted of virus without CBD and exposed to the same conditions. Subsequently, the mixtures were diluted 1:100 and 1:1000 with PBS and titrated by plaque assay.

Quantitative reverse transcription polymerase chain reaction

Vero and Huh-7 cells were infected with ZIKV and treated with concentrations of 5 and 10 μM of CBD during 48 h. RNA was extracted from cell cultures using the TRI Reagent® MRC from Molecular Research Center, Inc., and quantified by spectrophotometry (NanoDrop 2000; ThermoFisher Scientific). cDNA was synthesized using the Moloney murine leukemia virus reverse transcriptase and quantitative polymerase chain reaction (qPCR) was performed using FastStart™ Universal SYBR® Green Master (Rox) in a Bio-Rad iCycler with MyiQ2 Two-Color reverse transcription-PCR Detection System. Gene expression was normalized to the endogenous gene control Actin. Data were analyzed using the threshold cycle method ($2^{-\Delta\Delta Ct}$). The primers used were the following: actin (forward: 5′-TTA GTT GCG TTA CAC CCT TTC TTG-3′; reverse: 5′-TCA CCT TCA CCG TTC CAG TTT-3′); ZIKV (forward: 5′-GCC GCC ACC AAG ATG AAC TGA TTG-3′; reverse: 5′-GCA GTC

AU9 ▶ TCC CGG ATG CTC CAT C-3′); IFN-β (forward: 5′-TAG CAC TGG CTG GAA TGA GA-3′; reverse: 5′-
AU0 ▶ TCC TTG GCC TTC AGG TAA TG-3′).

Immunofluorescence assay

Vero cell cultures were grown on coverslips inserted on 24-well microplate during 24 h. After this time, cells were infected with ZIKV (MOI = 0.1) for 1 h and treated with 10 μM CBD for 48 h. To study viral infection, cells were fixed with ice-cold 100% methanol at −20°C for 10 min. Two types of antibodies were used to mark infected cells, anti-double-stranded RNA (anti-dsRNA) (1/100) (SCICONS; mAb J2) and anti-E protein (1/300) (Abcam). Cells were incubated for 1 h. Afterward, samples labeled with anti-E protein were incubated for 1 h with the anti-mouse IgG Alexa Fluor 488 secondary antibody (1/300) (Invitrogen). Regarding the cells marked with anti-dsRNA, the secondary antibody used was anti-rabbit IgG Alexa Fluor 488 (1/300) (Invitrogen). Finally, slides were stained with 4′,6-diamidino-2-phenylindole (DAPI; 1/1000) (Sigma-Aldrich Co.) for 10 min.

On the contrary, cell membranes were marked using Wheat Germ Agglutinin (WGA) conjugated with tetramethyl rhodamine isothiocyanate (TRITC) (Sigma-Aldrich Co.). Two different fixing solutions were used, ice-cold 100% methanol and 4% PFA followed by permeabilization with 0.1% Triton X-100. Cells were incubated with WGA-TRITC for 1 h at 37°C in a humid chamber. Subsequently, in the case of the cells that were infected, they were marked with the anti-dsRNA or with the anti-E protein antibodies, as mentioned above. Finally, nuclei staining was carried out with DAPI for 10 min. The coverslips of all samples were mounted on glass microscopy slides. The samples were visualized with an Olympus IX71 epifluorescence microscope and a Zeiss LSM 980 confocal microscope equipped with the Airyscan 2 super resolution module.

Cholesterol measurement

Total cholesterol (CHO) from infected and uninfected cell cultures was determined. For this, Vero cells were grown in 96-well plates and incubated for 24 h. After reaching 80% confluence, cells were infected with ZIKV and DENV-2 (MOI = 0.1). These infected cells and uninfected cells were treated with concentrations of 5 and 10 μM CBD for 48 h. Total CHO was measured using the Amplex™ Red Cholesterol Assay Kit (Invitrogen) following the manufacturer's instructions.

Statistical analysis

Experimental comparisons were made using Student's *t*-test in the case of two-group comparisons or the one-way analysis of variance (ANOVA) test for multiple comparisons.

ANOVA followed by Tukey's *post hoc* test was used ◀ AU10
when comparing was made between different groups or a one-way ANOVA followed by Dunnett's *post hoc* test when comparing was made every mean to a control mean. A p-value < 0.05 was considered significant. All experiments were performed in triplicate and data analysis was carried out with GraphPad Prism 8 software (San Diego, CA, USA).

Results

CBD inhibits ZIKV *in vitro* infection in relevant cellular models

First, we evaluated the cytotoxicity of CBD in different cell types relevant in the pathogenesis of ZIKV. Different human cell lines (Swan-71, NPCs, Huh-7, and ARPE-19 cells) were exposed to different dilutions of the phytochemical during 72 h and then determined cell viability by the MTT reduction assay. Results indicated that 20 μM CBD significantly induced cytotoxicity in Huh-7 and ARPE-19 cells versus nontreated cells (control) with cell viability values of 31.52% and 18.20%, respectively. However, at 10 μM CBD, cell viability values were above 90% and statistically not significantly different versus control cells. To note, regarding to NPCs and Swan-71 cells, viability was not affected at 20 μM CBD, but was considerably reduced at 40 μM (Fig. 1b). The 50% cytotoxic concentrations (CC50) are found in Table 1. ◀ T1

Based on the obtained data, we established the concentration range between 0.6 and 10 μM to study the CBD antiviral properties in the Huh-7 and ARPE-19. Particularly, the CBD antiviral activity was also tested in NPCs and Swan-71 cells at a concentration of 20 μM, since in these cases, the viability was $> 90\%$. As it is shown in Figure 1c, CBD exhibited a potent antiviral activity against ZIKV in the different cell cultures used with effective concentration 50% (EC50) values ranging from 1.40 to 5.12 μM (Table 1).

CBD inhibits other flaviviruses

To expand our study, we included the antiviral activity evaluation of CBD against two other flaviviruses, DENV-2 and YFV. To note, CBD was found to have a significant antiviral activity against these viruses. As

Table 1. Cytotoxicity and Antiviral Effect of Cannabidiol in Vero, Huh-7, ARPE-19, Swan-71 A549 Cells, and Neural Progenitor Cells

		EC50 (μM)							
Cell line	CC50 (μM)	ZIKV	DENV-2	YFV	CHIKV	HSV-1	JUNV	PV-1	ADV-5
Vero	16.10±0.28	0.87±0.28	2.02±0.31	2.13±0.32	4.63±0.47	8.27±0.51	8.55±0,22	4.88±0.076	ND
Huh-7	17.11±0.42	1.40±0.04	1.47±0.04	1.68±0.42	ND	4.46±0.201	8.50±0.52	4.24±0.26	ND
ARPE-19	15.73±0.46	2.01±0.05	ND	ND	ND	ND	ND	ND	ND
NPCs	30.90±1.18	3.23±0.17	ND	ND	ND	ND	ND	ND	ND
Swan-71	>40	5.12±1.20	ND	ND	ND	ND	ND	ND	ND
A549	15.99±0.49	ND	ND	ND	ND	ND	ND	ND	1.12±0.22

ADV-5, adenovirus type 5; CC50, 50% cytotoxicity concentration values were measured for noninfected cells; CHIKV, chikungunya virus; DENV-2, dengue virus, serotype 2; EC50, half maximal effective concentration values for cells infected with the indicated viruses; HSV-1, herpes simplex type 1; JUNV, Junín virus; ND, nondetermined; NPCs, neural progenitor cells; PV-1, poliovirus type 1; YFV, yellow fever virus; ZIKV, Zika virus.

F2 ▶ seen in Figure 2, DENV-2 and YFV both showed a significant inhibition of virus yield in Huh-7 cell culture after CBD treatment, even at lower concentrations (0.6–1.25 μM).

CBD increases the expression of IFN-β

To study the possible immunomodulatory role of CBD, we measured the levels of cytokines that play a key role in the innate response during viral infections. We determined the IL-6, IL-8, and IFN-β production in Huh-7 cells that were exposed to 10 μM CBD during 48 h. The results showed that 10 μM CBD-treated cells exhibited a significantly IFN-β F3 ▶ increased levels after 48 h (Fig. 3a), meanwhile, IL-6 and IL-8 were not induced (Fig. 3b, c). These results suggested that CBD has a partial immunomodulatory role.

Subsequently, to analyze whether the observed CBD antiviral effect was due solely to the modulation of IFN-β, the antiviral activity against flaviviruses was evaluated in Vero cell cultures. These cells are characterized by not producing IFN-I due to spontaneous genetic deletions. The cell viability was measured (Fig. 3d), and different concentrations were evaluated against ZIKV, DENV, and YFV. Surprisingly, it was observed a significant inhibition of viral yields after treatments of Vero-infected cell cultures, even at low CBD concentrations tested (0.6–1.2 μM) (Fig. 3e). Collectively, these results suggest that the antiviral effect exerted by CBD is independent of the IFN signaling pathway.

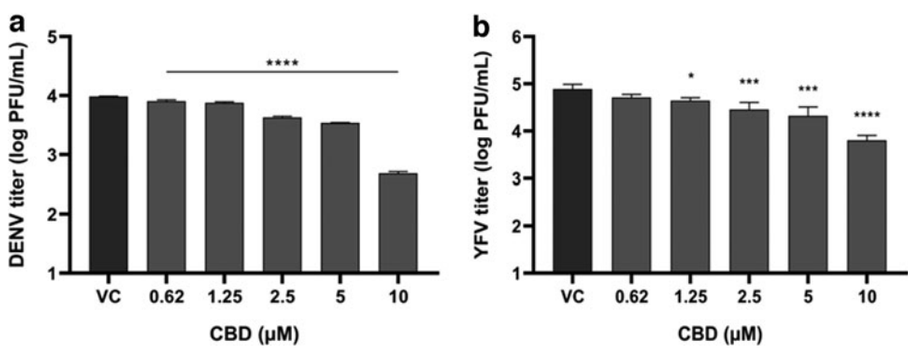

FIG. 2. Antiviral activity of CBD against **(a)** DENV-2 (MOI = 0.1) and **(b)** YFV (MOI = 0.1) in Huh-7 cell line. Cells were infected and treated at CBD concentrations of 0.6 to 10 μM during 48 h. Subsequently, the supernatants were harvested and titrated by the plaque assay in Vero cells. Viral control (VC): untreated and infected cells. Results are expressed as the mean ± SD ($n = 3$). *p*-Values were determined using an ANOVA analysis, followed by Dunnett's *post hoc* test. ****$p < 0.0001$, ***$p < 0.001$, *$p < 0.05$ versus VC. DENV-2, dengue virus, serotype 2; YFV, yellow fever virus.

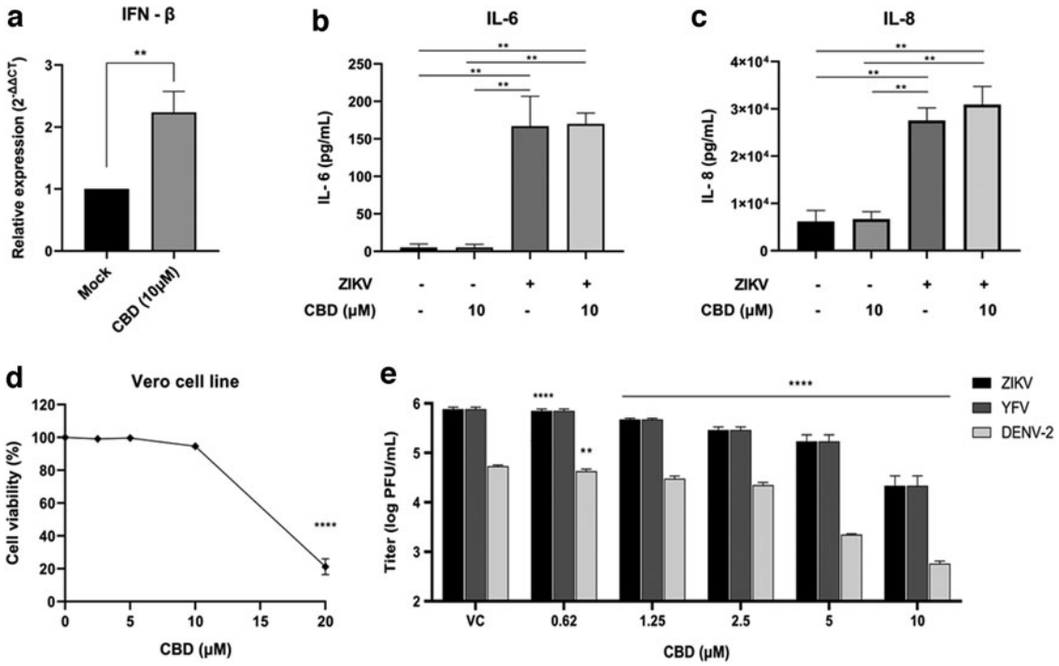

FIG. 3. Immunomodulatory role of CBD. **(a)** IFN-β mRNA expression in Huh-7 cells determined by qPCR. Expression values are relative to untreated cells. *p*-Values were determined by Student's *t*-test. $^{**}p < 0.01$. **(b, c)** ELISA quantification of IL-6 and IL-8 in supernatants of ZIKV-infected and treated with 10 μM CBD during 48 h. Data represent the mean ± SD ($n = 3$). *p*-Values were determined by a one-way ANOVA followed by Tukey's *post hoc* test. $^{**}p < 0.01$. **(d)** Cell viability of the Vero cell line. Cells were exposed to CBD concentrations from 2.5 to 20 μM for 72 h. Subsequently, the viability was determined by the MTT method. **(e)** CBD's antiviral properties against ZIKV, DENV-2, and YFV (MOI = 0.1) in Vero cells. After infection, cells were exposed to different CBD concentrations (0.6–10 μM) for 48 h. Infectious particles were quantified by the plaque assay. Mock: untreated and uninfected cells. Viral control (VC): untreated and infected cells. *p*-Values were determined by a one-way ANOVA followed by Dunnett's *post hoc* test. $^{****}p < 0.0001$, $^{**}p < 0.01$ versus VC. ELISA, enzyme-linked immunosorbent assay; IFN-β; IL, interleukin; MOI, multiplicity of infection; qPCR, quantitative polymerase chain reaction.

CBD inhibits chikungunya virus

Usually, flaviviruses cocirculate in the same areas as CHIKV that belongs to the Togaviridae family. Thus, we evaluated the CBD antiviral activity against this nonrelated arbovirus. The obtained results showed that there was a significant reduction of infectious foci at concentrations of 2.5, 5, and 10 μM (Fig. 4), resulting in an EC50 of 4.63 μM (Table 1).

CBD impacts at different viral replication stages

To get some insight about viral replication stages affected by CBD, an addition time assay was carried out on the Huh-7 cell line. For this purpose, cells were infected and 10 μM CBD was added at 0, 2, 4, 6, and 8 hpi. As Figure 5a shows, a significant inhibition was observed mainly in the first 2 h of infection. In an attempt to determine whether CBD had a direct virucidal effect, a viral inactivation assay was performed. For this purpose, ZIKV was exposed to CBD concentrations of 5 and 10 μM for 1 h at 37°C. Subsequently, the mixtures were titrated by the plaque assay.

Notably, CBD did not present a virucidal effect, since no differences in quantification of viral particles was observed after treatment (Fig. 5b). Therefore, the inhibition of the first hours suggests that CBD might interfere with early interactions between the virion and the

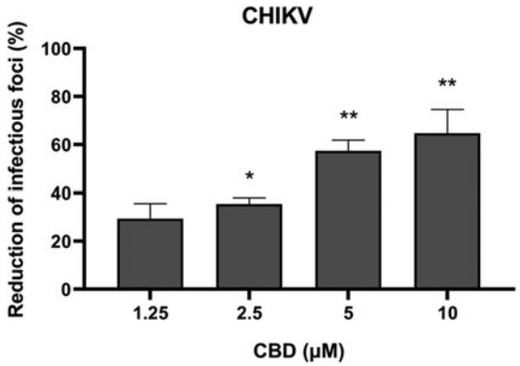

FIG. 4. Antiviral activity of CBD against CHIKV. Vero cells infected with CHIKV-ZsGreen (MOI = 0.02) were treated with CBD (1.25–10 μM) and after 20 h of incubation, fixed with 4% PFA. The infectious foci were quantified by the ELISpot equipment. *p*-Values were determined by a one-way ANOVA followed by Dunnett's *post hoc* test. $^{**}p < 0.01$, $^{*}p < 0.05$ versus infected and untreated cells. CHIKV-ZsGreen, chikungunya virus expressing ZsGreen fluorescent protein; PFA, paraformaldehyde.

host cell, mainly during both adsorption and internalization stages. Surprisingly, when this assay was performed in Vero cells (Fig. 5c), it was observed a significant inhibition in the intermediate (viral genome replication and translation) and late viral stages (assembly, processing, and virions release) ($t = 4, 6, 8$ hpi).

On the contrary, the relative RNA viral level in ZIKV-infected Huh-7 and Vero cell cultures was quantified by qPCR. The obtained results demonstrated that there was a significant decrease in the relative expression of viral RNA when the infected cell cultures were treated with 5 and 10 μM of CBD (Fig. 5d, e) in comparison to viral control.

Based on these results, the percentage of infected cells was determined by confocal microscopy imaging quantification. Vero cells infected with ZIKV and treated with 10 μM CBD for 48 h were fixed and labeled with anti-dsRNA or anti-E protein antibodies, as indicated in the Figure 5f–i. dsRNA is produced as an intermediate in the RNA synthesis during the genome replication of many viruses, including flaviviruses. In comparison to the viral control, a significant inhibition of infected cells was found after the treatments (Fig. 5f–i). The results observed in the cells stained with anti-dsRNA corroborated what was determined by qPCR, a significant reduced quantity of viral RNA was detected (Fig. 5g).

However, when E viral antigen was detected, almost a complete inhibition was observed compared to the control (Fig. 5i). These results suggest that although the virions are able to infect a considerable number of cells in the presence of CBD treatment (dsRNA staining), the protein translation is mainly affected (E staining). These results were in accordance with those depicted in Figure 5c, in which at different time of CBD addition a significant inhibition was observed; however, the most affected viral steps were the intermediate and late ones.

FIG. 5. **(a, c)** Addition of CBD at different times postinfection in **(a)** Huh-7 and **(c)** Vero cells. Cells were infected with ZIKV (MOI = 0.5) and 10 μM of CBD were added at 0, 2, 4, 6, and 8 hpi. Supernatant were collected at 24 hpi and titrated by the plaque assay. **(b)** Virucidal effect of CBD against ZIKV (MOI = 0.5). The virus was exposed to 10 and 5 μM CBD for 1.30 h at 37°C. Subsequently, the mixtures were diluted and titrated by the plaque assay. **(d, e)** Viral RNA levels determined by qPCR in **(d)** Huh-7 cells and **(e)** Vero cells. Data represent the mean ± SD ($n = 3$). *p*-Values were determined by a one-way ANOVA followed Dunnett's *post hoc* analysis. $^{****}p < 0.0001$, $^{***}p < 0.001$, $^{**}p < 0.01$, $^{*}p < 0.05$ versus VC. **(f–i)** ZIKV infection visualized by immunofluorescence. Cells were infected with ZIKV (MOI = 0.1) and afterward treated with 10 μM CBD. Cell cultures were fixed with methanol and labeled with **(f)** anti-dsRNA antibody and **(g)** anti-E protein antibody. Alexa 488 (green) was used as the secondary antibody. **(g, i)** Images of random fields of view were acquired to determine the number of infected cells. The green fluorescence of each cell was quantified to measure the intensity of infection and subsequently, an average was calculated. The samples were visualized with an Olympus IX71 epifluorescence microscope. Cell quantification and fluorescence intensity measurement was performed using Fiji software. Viral control (VC): untreated infected cells. *p*-Values were calculated by Student's *t*-test. Data represent the mean ± SD ($n = 3$). $^{****}p < 0.0001$, $^{**}p < 0.01$ versus VC. dsRNA, double-stranded RNA; hpi, hours postinfection.

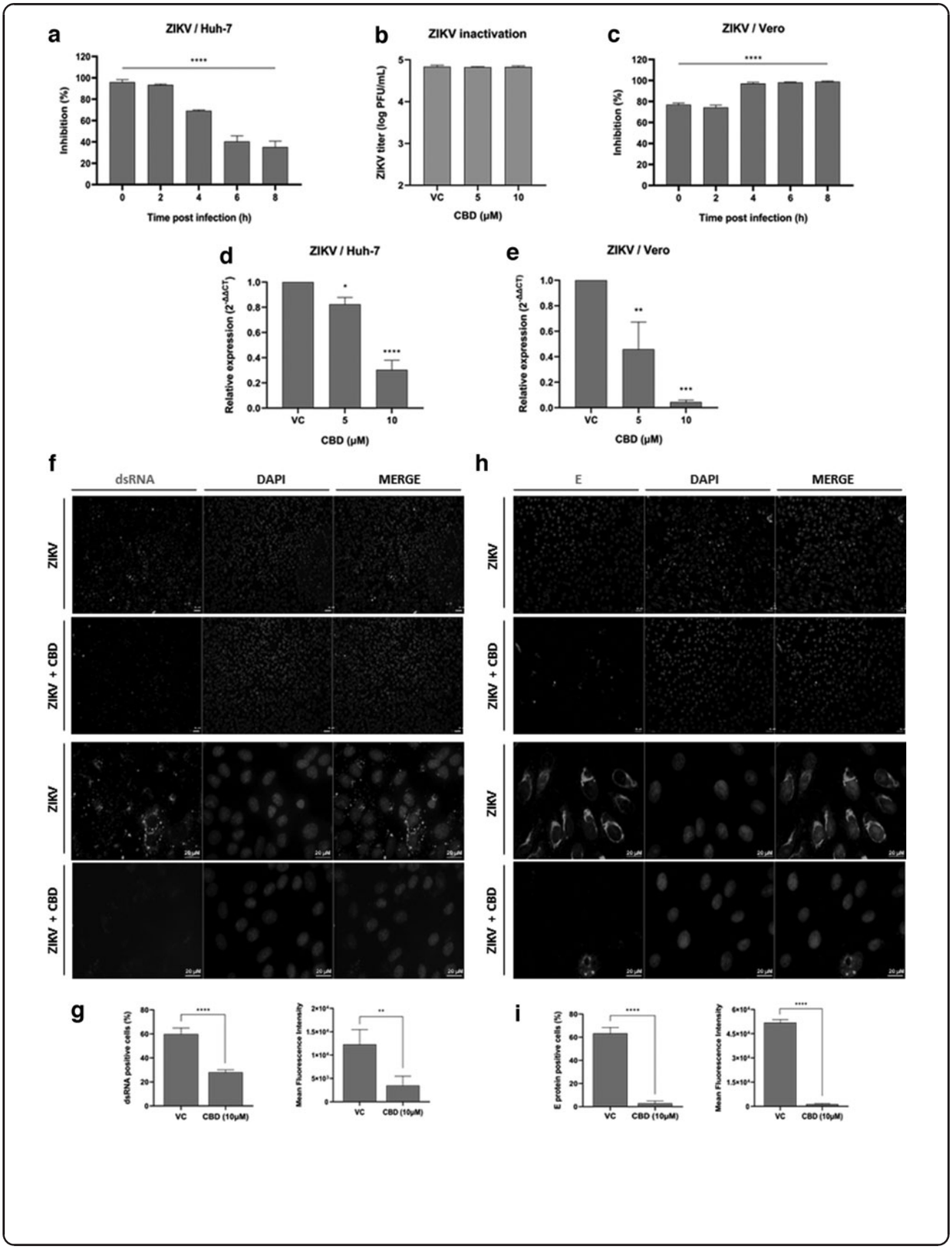
a
ZIKV / Huh-7
Inhibition (%)
Time post infection (h)
b
ZIKV inactivation
ZIKV titer (log PFU/mL)
CBD (µM)
c
ZIKV / Vero
Inhibition (%)
Time post infection (h)
d
ZIKV / Huh-7
Relative expression (2-ΔΔCT)
CBD (µM)
e
ZIKV / Vero
Relative expression (2-ΔΔCT)
CBD (µM)
f
dsRNA
DAPI
MERGE
ZIKV
ZIKV + CBD
h
E
DAPI
MERGE
g
dsRNA positive cells (%)
Mean Fluorescence Intensity
VC
CBD (10µM)
i
E protein positive cells (%)
Mean Fluorescence Intensity

CBD alters cellular membranes impacting ZIKV infection

The flavivirus replication cycle is highly cell membrane dependent. This involves from the entry and exit of the virion to the cell by endocytosis and exocytosis, respectively, to the synthesis of RNA, assembly processing and transport of the particles in the endoplasmic reticulum (ER) and Golgi membranes.[26–29] To study the impact of CBD on cell membranes in the context of ZIKV infections, treatments were performed on uninfected and infected Vero cells with 10 μM of CBD for 48 h.

Afterward, cells were fixed under different conditions, PFA to preserve cellular membranes or methanol to explore intracellular membranes (ER/Golgi). Then, samples were labeled with WGA, a lectin that binds nonenzymatically to N-acetyl-D-glucosamine and sialic acid residues of glycoproteins and glycolipids present in the plasmatic membrane, ER and Golgi, and observed in detail by high-resolution confocal microscopy. Images were analyzed and fluorescence intensity quantified, revealing that uninfected and infected CBD-treated samples exhibited an increase in fluorescence intensity, suggesting that CBD modifies cell membranes (Fig. 6).

CHO, one of the main components of the plasma membrane, maintains the integrity of the membrane, regulates its fluidity, and plays an important role in the formation of lipid rafts. As mentioned above, cell membranes are highly important in the flavivirus replication cycle. The lipid rafts containing a high CHO content are a key area of virion entry and budding.[30] In addition, the proteins involved in the synthesis and regulation of CHO are anchored in the ER membranes.[31,32] On the contrary, the relationship between CHO and the IFN-I response during viral infections is also significant, as excessive CHO levels are known to impair IFN responsiveness.[33]

Hence, a decrease in CHO amount during a flavivirus infection may ensure an improvement in the IFN's response. Therefore, we performed a measurement of cellular CHO in CBD-treated Vero cells, uninfected or ZIKV and DENV-2 infected. The results showed that in all conditions, there was a reduction in CHO levels after CBD treatment (Fig. 6e–g). Collectively, these results indicate that CBD decreases cellular CHO, which alters cell membranes and, consequently, affects both ZIKV and DENV-2 viral replication.

CBD is a broad-spectrum antiviral

Finally, to broaden the antiviral spectrum of CBD, structurally unrelated viruses that cause serious infections in humans were subjected to study. For this, cells were infected with enveloped viruses such as HSV-1 and JUNV and nonenveloped viruses such as PV-1 and ADV-5. Furthermore, these viruses differ widely in their genome composition (DNA vs. RNA genome). Vero and Huh-7 cell lines were used for the HSV-1, JUNV, and PV-1 viruses and A549 for ADV-5 since it represents an optimal replication system for the latter virus.

FIG. 6. Labeling pattern of cell membranes in Vero cells using confocal fluorescence microscopy. Infected (ZIKV) and uninfected (Mock) cells were treated with 10 μM CBD for 48 h. Subsequently, they were fixed with different solvents, the membranes were stained with WGA-TRITC (red) and viral antigens (green). **(a)** Cells fixed with 4% PFA and permeabilized with 0.1% Triton X-100. Infected cells were labeled with the primary anti-dsRNA antibody and then, with the secondary antibody Alexa 488. **(b)** Quantification of WGA-TRITC fluorescence intensity per cell of infected and uninfected cells fixed with 4% PFA. **(c)** Cells fixed with absolute methanol, labeled with the primary antibody anti-E protein and the secondary antibody Alexa 488. **(d)** Quantification of fluorescence WGA-TRITC intensity per cell of infected and uninfected cells fixed with absolute methanol. The samples were visualized under the Zeiss LSM 980 confocal microscope. Intensity quantifications were performed with the Fiji software. *p*-Values were calculated by Student's *t*-test. Data represent the mean ± SD ($n = 3$). ****$p < 0.0001$, ***$p < 0.001$, **$p < 0.01$ versus control. **(e–g)** Intracellular CHO quantification in Vero cells. Cells were treated with CBD concentrations of 5 and 10 μM for 48 h and then, CHO was quantified by a fluorimetric method. **(e)** Uninfected cells; **(f)** Cells infected with ZIKV (MOI = 0.1); **(g)** Cells infected with DENV-2 (MOI = 0.1). Mock: untreated and uninfected cells. Viral control (VC): untreated and infected cells. *p*-Values were determined by a one-way ANOVA followed by Dunnett's *post hoc* test. Data represent the mean ± SD ($n = 3$). ***$p < 0.001$, *$p < 0.05$. CHO, cholesterol; WGA-TRITC, Wheat Germ Agglutinin-tetramethyl rhodamine isothiocyanate.

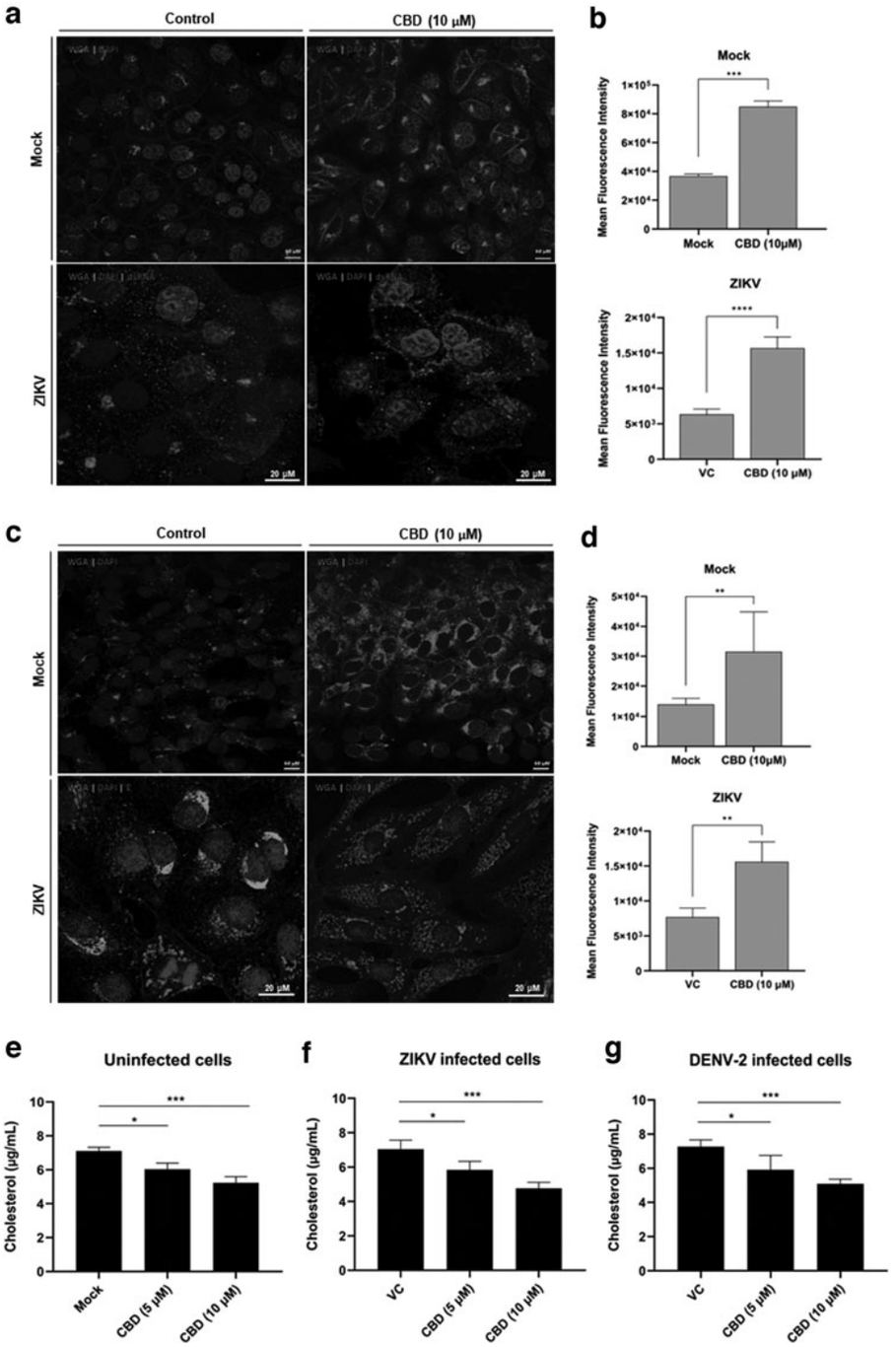
a
Control
CBD (10 μM)
Mock
ZIKV
20 μM
b
Mock
Mean Fluorescence Intensity
Mock
CBD (10μM)
ZIKV
VC
CBD (10 μM)
c
d
e
Uninfected cells
Cholesterol (μg/mL)
Mock
CBD (5 μM)
CBD (10 μM)
f
ZIKV infected cells
VC
g
DENV-2 infected cells

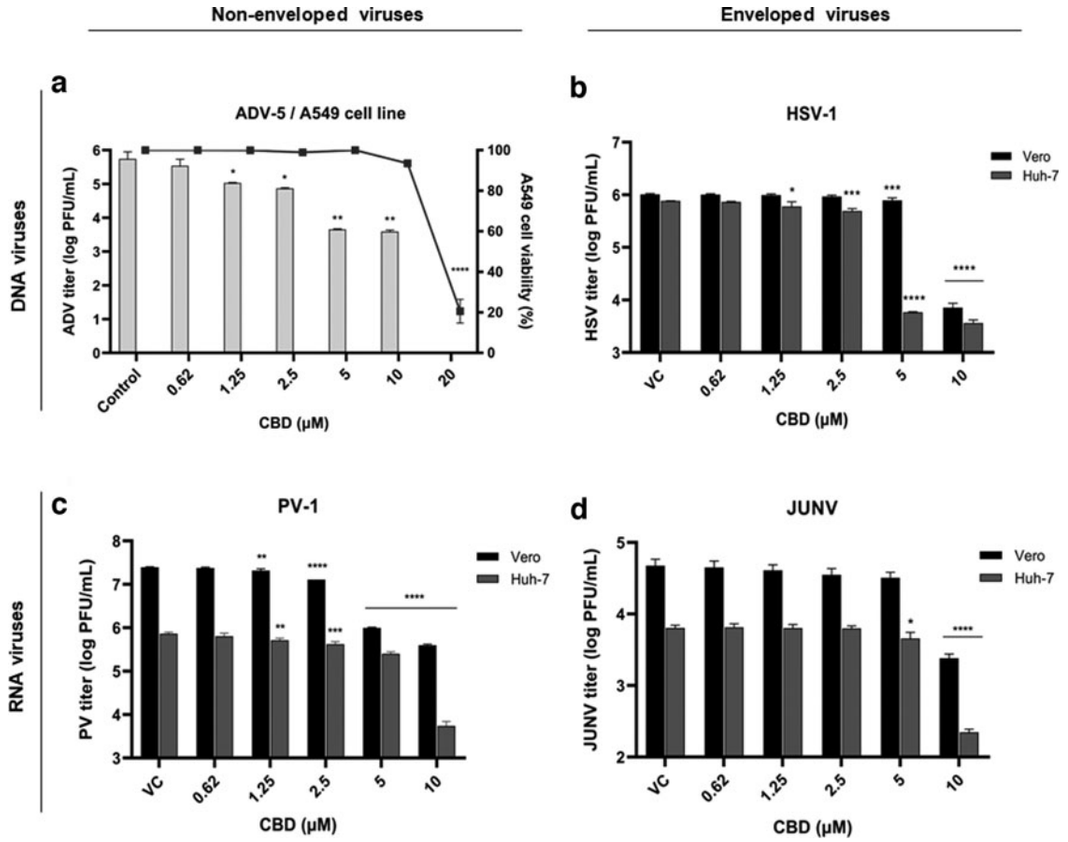

FIG. 7. Antiviral activity of CBD against structurally dissimilar viruses. Cells were infected for 1 h and subsequently treated with CBD (0.6–10 μM) for 24 h in the case of PV-1 and 48 h for the other viruses. The supernatants were harvested, and the viral titers were determined by the plaque assay. **(a)** ADV-5 (MOI = 0.1). Cell viability of the A549 cell line was determined. For this, cells were exposed to a concentration range of CBD from 0.6 to 20 μM for 72 h. Subsequently, viability was determined by the MTT assay. **(b)** HSV-1 (MOI = 0.07); **(c)** PV-1 (MOI = 0.07); **(d)** JUNV (MOI = 0.1). Viral control (VC): untreated infected cells. *p*-Values were determined by a one-way ANOVA followed by Dunnett's *post hoc* test. Data represent the mean ± SD ($n = 3$). ****$p < 0.0001$, ***$p < 0.001$, **$p < 0.01$ and *$p < 0.05$ versus control. ADV-5, adenovirus type 5; HSV-1, herpes simplex type 1; JUNV, Junín virus; PV-1, poliovirus type 1.

Subsequently, treatments with CBD were carried out in a concentration range of 0.6 to 10 μM. The results indicated that CBD significantly inhibited all virus replication at a concentration of 10 μM. In the case of HSV-1, PV-1, and ADV-5, a significant inhibition of up to 1.25 μM was observed (Fig. 7). Regarding the results obtained using both different cell lines, no major differences were observed as occurred with the flaviviruses.

The EC50 and CC50 obtained in all mentioned experiments performed are summarized in Table 1.

Discussion and Conclusions

In the present work, especial focus on the evaluation of CBD anti-ZIKV activity was made. The ZIKV infection has been associated with severe complications and adverse effects on the fetus, mainly during the first trimester of pregnancy.[34,35] This flavivirus crosses the placenta infecting trophoblast cells and reaches the fetal brain where the virus mainly infects NPCs.[36–38] This infection seriously affects the brain development of the fetus that might generate severe conditions such as microcephaly. In addition, ZIKV infects other

highly relevant cellular targets such as liver cells and retinal pigment epithelium cells.[39–41] By using different cellular models relevant to the viral pathogeny, our results suggest a potential application of CBD to treat ZIKV and other flaviviruses such as DENV and YFV, and a nonrelated but not less important arbovirus, such as CHIKV, that cocirculates in same affected area.

In recent works, the immunomodulatory role of CBD during SARS-CoV-2 infections has been closely studied, determining that CBD increases the expression of interferon and upregulates its signaling pathway.[19] On the contrary, a recent study showed that CBD administration reduced the level of proinflammatory cytokines (e.g., IL-6, IFN-γ) and improved clinical symptoms of acute respiratory distress syndrome in a murine model.[42] In addition, it has been reported that CBD inhibits polymorphonuclear leukocytes migration and the production of reactive oxygen species and TNF-α.[43] In line with these observations, we determined that, although CBD induces the expression of IFN-β, the main antiviral effect involves another mechanism.

Recently, it has been proposed that one of the steps affected by the action of CBD in cells infected by SARS-CoV-2 is the cell entry.[19,44,45] In accordance with that observation, the inhibition of ZIKV infection during the first hours suggests that CBD might interfere with early interactions between the virion and the host cell. Nonetheless, our results also revealed that intermediate viral stages as protein translation are significantly affected.

It is well known that CBD affects the integrity and physicochemical properties of cell membranes such as fluidity, permeability, and elasticity.[46–48] Newly, a growing interest in the relationship between CHO and CBD has emerged. *In vitro* studies have shown that after incubation with CBD, CBD localizes to cell membranes, interacts with phospholipids, and interferes with normal CHO distribution; as a consequence, the permeability of the membrane undergoes modifications.[46,49] In the present report, CBD significantly diminished total cellular CHO levels. This finding suggests that this alteration impacts directly on viral replication.

During last decades, different global viral outbreaks systematically have emerged and remerged (SARS-CoV-1, SARS-CoV-2, MERS-CoV, ZIKV, DENV, Influenza A H1N1 2009 and Ebola).[50] With this, the need to generate greater scientific and economic efforts in the search for broad-spectrum antivirals is exposed. In particular, the repurposing of drugs already tested in humans is highly desirable in terms of time and cost savings and is therefore a valuable alternative in emergency situations during public health crises.

In conclusion, we give hope to the use of CBD by demonstrating the *in vitro* effectiveness of the CBD as a broad-spectrum antiviral molecule that can be used against different dissimilar viruses. However, future studies are necessary to confirm this proof of principle of CBD as an antiviral in animal models.

Acknowledgments

The authors thank all members of the laboratories involved for helpful advice and discussions.

Authors' Contributions

A.M. carried out the experiments and data analysis - writing. J.V. performed the quantifications of IL-6 and IL-8 by ELISA. C.B. supervised these experiments. E.C. carried out the antiviral tests against chikungunya. D.A. supervised these experiments. D.V. preparation of plates and maintenance of Swan-71 cells. M.S.R.-V. preparation of plates and maintenance of NPCs cultures. L.R. supervised this work. G.M.F. performed the extraction and column chromatography purification. A.P. and P.A.L.C. collaborated on the purification and characterization. C.R. designed and conducted the experiments for the extraction and purification, and performed the HPLC characterization. A.A., review the whole research. C.G., designed and led the whole research - writing, review, and editing. All authors have read and agreed to the published version of the article.

Disclaimer

The funders had no role in the design of the study; in the collection, analyses, or interpretation of data; in the writing of the article; or in the decision to publish the results.

Author Disclosure Statement

The authors declare no conflict of interest.

Funding Information

This work was funded by Universidad de Buenos Aires (UBA) (grant number 20020170100363BA) and Consejo Nacional de Investigaciones Científicas y Tecnológicas (CONICET) (grant number 11220210100168CO). E.C., D.V., P.A.L.C., A.P., L.R., D.A., C.B., C.R., A.A., and C.G. are members of the Research Career from CONICET; A.M., J.V., and M.S.R.-V. are fellows from CONICET.

AU12 ▶ ## References

1. Newman DJ, Cragg GM. Natural products as sources of new drugs from 1981 to 2014. J Nat Prod 2016;79(3):629–661; doi: 10.1021/acs.jnatprod.5b01055
2. Cragg GM, Newman DJ. Biodiversity: A continuing source of novel drug leads. Pure Appl Chem 2005;77(1):7–24; doi: 10.1351/pac200577010007
3. Sea YL, Gee YJ, Lal SK, et al. Cannabis as antivirals. J Appl Microbiol 2023; 134(1):1–13; doi: 10.1093/jambio/lxac036
4. Atalay S, Jarocka-Karpowicz I, Skrzydlewska E. Antioxidative and anti-inflammatory properties of cannabidiol. Antioxidants (Basel) 2019;9(1); doi: 10.3390/antiox9010021
5. Fiani B, Sarhadi KJ, Soula M, et al. Current application of cannabidiol (CBD) in the management and treatment of neurological disorders. Neurol Sci 2020;41(11):3085–3098; doi: 10.1007/s10072-020-04514-2
6. Campos AC, Fogaça MV, Sonego AB, et al. Cannabidiol, neuroprotection and neuropsychiatric disorders. Pharmacol Res 2016;112:119–127; doi: 10.1016/j.phrs.2016.01.033
7. Silvestro S, Mammana S, Cavalli E, et al. Use of cannabidiol in the treatment of epilepsy: Efficacy and security in clinical trials. Molecules 2019; 24(8); doi: 10.3390/molecules24081459
8. Zhang X, Qin Y, Pan Z, et al. Cannabidiol induces cell cycle arrest and cell apoptosis in human gastric cancer SGC-7901 cells. Biomolecules 2019; 9(8); doi: 10.3390/biom9080302
9. Hamad H, Olsen BB. Cannabidiol induces cell death in human lung cancer cells and cancer stem cells. Pharmaceuticals (Basel) 2021;14(11); doi: 10.3390/ph14111169
10. Huang T, Xu T, Wang Y, et al. Cannabidiol inhibits human glioma by induction of lethal mitophagy through activating TRPV4. Autophagy 2021; 17(11):3592–3606; doi: 10.1080/15548627.2021.1885203
11. Shangguan F, Zhou H, Ma N, et al. A novel mechanism of cannabidiol in suppressing hepatocellular carcinoma by inducing GSDME dependent pyroptosis. Front Cell Dev Biol 2021;9:697832; doi: 10.3389/fcell.2021.697832
12. Durst R, Danenberg H, Gallily R, et al. Cannabidiol, a nonpsychoactive cannabis constituent, protects against myocardial ischemic reperfusion injury. Am J Physiol Heart Circ Physiol 2007;293(6):H3602–H3607; doi: 10.1152/ajpheart.00098.2007
13. Garza-Cervantes JA, Ramos-González M, Lozano O, et al. Therapeutic applications of cannabinoids in cardiomyopathy and heart failure. Oxid Med Cell Longev 2020;2020:4587024; doi: 10.1155/2020/4587024
14. Mabou Tagne A, Pacchetti B, Sodergren M, et al. Cannabidiol for viral diseases: Hype or hope? Cannabis Cannabinoid Res 2020;5(2):121–131; doi: 10.1089/can.2019.0060
15. Lowe H, Toyang N, McLaughlin W. Potential of cannabidiol for the treatment of viral hepatitis. Pharmacognosy Res 2017;9(1):116–118; doi: 10.4103/0974-8490.199780
16. Tomer S, Mu W, Suryawanshi G, et al. Cannabidiol modulates expression of type I IFN response genes and HIV infection in macrophages. Front Immunol 2022;13:926696; doi: 10.3389/fimmu.2022.926696
17. DeMarino C, Cowen M, Khatkar P, et al. Cannabinoids reduce extracellular vesicle release from HIV-1 infected myeloid cells and inhibit viral transcription. Cells 2022;11(4); doi: 10.3390/cells11040723
18. Nguyen LC, Yang D, Nicolaescu V, et al. Cannabidiol inhibits SARS-CoV-2 replication and promotes the host innate immune response. bioRxiv 2021; doi: 10.1101/2021.03.10.432967
19. Nguyen LC, Yang D, Nicolaescu V, et al. Cannabidiol inhibits SARS-CoV-2 replication through induction of the host ER stress and innate immune responses. Sci Adv 2022;8(8); doi: 10.1126/sciadv.abi6110
20. Corpetti C, Del Re A, Seguella L, et al. Cannabidiol inhibits SARS-Cov-2 spike (S) protein-induced cytotoxicity and inflammation through a PPARγ-dependent TLR4/NLRP3/Caspase-1 signaling suppression in Caco-2 cell line. Phytother Res 2021;35(12):6893–6903; doi: 10.1002/ptr.7302
21. Nagarkatti P, Miranda K, Nagarkatti M. Use of cannabinoids to treat acute respiratory distress syndrome and cytokine storm associated with coronavirus disease-2019. Front Pharmacol 2020;11(November):1–6; doi: 10.3389/fphar.2020.589438
22. Beckham JD, Pastula DM, Massey A, et al. Zika virus as an emerging global pathogen: Neurological complications of Zika virus. JAMA Neurol 2016; 73(7):875–879; doi: 10.1001/jamaneurol.2016.0800
23. Faizan MI, Abdullah M, Ali S, et al. Zika virus-induced microcephaly and its possible molecular mechanism. Intervirology 2016;59(3):152–158; doi: 10.1159/000452950
24. Saingam W, Sakunpak A. Development and validation of reverse phase high performance liquid chromatography method for the determination of delta-9-tetrahydrocannabinol and cannabidiol in oromucosal spray from cannabis extract. Rev Bras Farmacogn 2018;28(6):669–672; doi: 10.1016/j.bjp.2018.08.001
25. Battini L, Fidalgo DM, Álvarez DE, et al. Discovery of a potent and selective Chikungunya virus envelope protein inhibitor through computer-aided drug design. ACS Infect Dis 2021;7(6):1503–1518; doi: 10.1021/acsinfecdis.0c00915
26. Smit JM, Moesker B, Rodenhuis-Zybert I, et al. Flavivirus cell entry and membrane fusion. Viruses 2011;3(2):160–171; doi: 10.3390/v3020160
27. Sánchez-San Martín C, Liu CY, Kielian M. Dealing with low pH: Entry and exit of alphaviruses and flaviviruses. Trends Microbiol 2009;17(11):514–521; doi: 10.1016/j.tim.2009.08.002
28. Morita E, Suzuki Y. Membrane-associated flavivirus replication complex: Its organization and regulation. Viruses 2021;13(6); doi: 10.3390/v13061060
29. Barnard TR, Abram QH, Lin QF, et al. Molecular determinants of flavivirus virion assembly. Trends Biochem Sci 2021;46(5):378–390; doi: 10.1016/j.tibs.2020.12.007
30. Peruzzu D, Amendola A, Venturi G, et al. Zika virus exploits lipid rafts to infect host cells. Viruses 2022;14(9); doi: 10.3390/v14092059
31. Jacquemyn J, Cascalho A, Goodchild RE. The ins and outs of endoplasmic reticulum-controlled lipid biosynthesis. EMBO Rep 2017;18(11):1905–1921; doi: 10.15252/embr.201643426
32. Volkmar N, Thezenas M-L, Louie SM, et al. The ER membrane protein complex promotes biogenesis of sterol-related enzymes maintaining cholesterol homeostasis. J Cell Sci 2019;132(2); doi: 10.1242/jcs.223453
33. Liu S-Y, Aliyari R, Chikere K, et al. Interferon-inducible cholesterol-25-hydroxylase broadly inhibits viral entry by production of 25-hydroxycholesterol. Immunity 2013;38(1):92–105; doi: 10.1016/j.immuni.2012.11.005
34. Freitas DA, Souza-Santos R, Carvalho LMA, et al. Congenital Zika syndrome: A systematic review. PLoS One 2020;15(12):e0242367; doi: 10.1371/journal.pone.0242367
35. Kafer D, Marquez A, Merech F, et al. Targeting first trimester trophoblast cell metabolism modulates its susceptibility to Zika virus infection. J Cell Physiol 2023;238(4):749–760; doi: 10.1002/jcp.30970
36. Nguyen HN, Qian X, Song H, et al. Neural stem cells attacked by Zika virus. Cell Res 2016;26(7):753–754; doi: 10.1038/cr.2016.68
37. Li H, Saucedo-Cuevas L, Regla-Nava JA, et al. Zika virus infects neural progenitors in the adult mouse brain and alters proliferation. Cell Stem Cell 2016;19(5):593–598; doi: 10.1016/j.stem.2016.08.005
38. Chiu C-F, Chu L-W, Liao I-C, et al. The mechanism of the Zika virus crossing the placental barrier and the blood-brain barrier. Front Microbiol 2020;11:214; doi: 10.3389/fmicb.2020.00214
39. Russo CA, Torti MF, Marquez AB, et al. Antiviral bioactivity of resveratrol against Zika virus infection in human retinal pigment epithelial cells. Mol Biol Rep 2021;48(7):5379–5392; doi: 10.1007/s11033-021-06490-y
40. Roach T, Alcendor DJ. Zika virus infection of cellular components of the blood-retinal barriers: Implications for viral associated congenital ocular disease. J Neuroinflammation 2017;14(1); doi: 10.1186/s12974-017-0824-7
41. Simonin Y, Erkilic N, Damodar K, et al. Zika virus induces strong inflammatory responses and impairs homeostasis and function of the human retinal pigment epithelium. EBioMedicine 2019;39:315–331; doi: 10.1016/j.ebiom.2018.12.010
42. Khodadadi H, Salles ÉL, Jarrahi A, et al. Cannabidiol modulates cytokine storm in acute respiratory distress syndrome induced by simulated viral infection using synthetic RNA. Cannabis Cannabinoid Res 2020;5(3):197–201; doi: 10.1089/can.2020.0043
43. Mabou Tagne A, Marino F, Legnaro M, et al. A novel standardized *Cannabis sativa* L. extract and its constituent cannabidiol inhibit human polymorphonuclear leukocyte functions. Int J Mol Sci 2019;20(8); doi: 10.3390/ijms20081833
44. Hoffmann M, Kleine-Weber H, Schroeder S, et al. SARS-CoV-2 cell entry depends on ACE2 and TMPRSS2 and is blocked by a clinically proven protease inhibitor. Cell 2020;181(2):271–280.e8; doi: 10.1016/j.cell.2020.02.052
45. Wang B, Kovalchuk A, Li D, et al. In search of preventive strategies: Novel high-CBD *Cannabis sativa* extracts modulate ACE2 expression in COVID-19 gateway tissues. Aging (Albany NY) 2020;12(22):22425–22444; doi: 10.18632/aging.202225

46. Perez E, Ceja-Vega J, Krmic M, et al. Differential interaction of cannabidiol with biomembranes dependent on cholesterol concentration. ACS Chem Neurosci 2022;13(7):1046–1054; doi: 10.1021/acschemneuro.2c00040
47. Atalay S, Dobrzyńska I, Gęgotek A, et al. Cannabidiol protects keratinocyte cell membranes following exposure to UVB and hydrogen peroxide. Redox Biol 2020;36:101613; doi: 10.1016/j.redox.2020.101613
48. Ghovanloo M-R, Choudhury K, Bandaru TS, et al. Cannabidiol inhibits the skeletal muscle Nav1.4 by blocking its pore and by altering membrane elasticity. J Gen Physiol 2021;153(5); doi: 10.1085/jgp.202012701
49. Mavromoustakos T, Daliani I. Effects of cannabinoids in membrane bilayers containing cholesterol. Biochim Biophys Acta 1999;1420(1–2):252–265; doi: 10.1016/S0005-2736(99)00106-6
50. Bhadoria P, Gupta G, Agarwal A. Viral pandemics in the past two decades: An overview. J Family Med Prim Care 2021;10(8).

Cite this article as: Marquez A, Vicente J, Castro E, Vota D, Rodríguez-Varela MS, Lanza Castronuovo PA, Fuentes GM, Parise A, Romorini L, Alvarez D, Bueno C, Ramirez C, Alaimo A, García C (2023) Broad-spectrum antiviral effect of cannabidiol against enveloped and non-enveloped viruses, *Cannabis and Cannabinoid Research* X:X, 1–15, DOI: 10.1089/can.2023.0103.

Abbreviations Used

Δ^9-THC = Δ-9-tetrahydrocannabinol
ADV-5 = adenovirus type 5
ANOVA = analysis of variance
bFGF = basic fibroblast growth factor
CBD = cannabidiol
CC50 = 50% cytotoxic concentrations
CHIKV-ZsGreen = chikungunya virus expressing ZsGreen fluorescent protein
CHO = cholesterol
DAPI = 4′,6-diamidino-2-phenylindole
DENV-2 = dengue virus, serotype 2
DMEM-F12 = Dulbecco's modified Eagle's medium and Nutrient Mixture F12
dsRNA = double-stranded RNA
EC50 = effective concentration 50%
EGF = epidermal growth factor
ELISA = enzyme-linked immunosorbent assay
ER = endoplasmic reticulum
FBS = fetal bovine serum
hpi = hours postinfection
HPLC =
HSV-1 = herpes simplex type 1
IFN =
IL-6 = interleukin-6
IL-8 = interleukin-8
JUNV = Junín virus
MEM = minimal essential medium
MOI = multiplicity of infection
MTT = 3-(4,5-dimethylthiazol-2-yl)-2,5-diphenyl tetrazolium bromide
NPCs = neural progenitor cells
PFA = paraformaldehyde
PV-1 = poliovirus type 1
qPCR = quantitative polymerase chain reaction
SARS-CoV-2 = severe acute respiratory syndrome coronavirus 2
TRITC = tetramethyl rhodamine isothiocyanate
WGA = Wheat Germ Agglutinin
YFV = yellow fever virus
ZIKV = Zika virus

◀ AU13
◀ AU14

AUTHOR QUERY FOR CAN-2023-0103-VER9-MARQUEZ_1P

AU0: The Publisher requests for readability that no paragraph exceeds 20 typeset lines. This paragraph contains 21 lines or more. Please divide where needed.
AU1: Please note that gene symbols in any article should be formatted per the gene nomenclature. Thus, please make sure that gene symbols, if any in this article, are italicized.
AU2: Please review all authors' surnames for accurate indexing citations. Please confirm all double surnames.
AU3: Please mention the degree abbreviation (e.g., MS, MD, PhD) of the corresponding author.
AU4: Please include the Clinical Trial Registration number, if applicable, at the end of the abstract.
AU5: Please provide a structural abstract.
AU6: Keywords have been taken from PDF. Please check.
AU7: Please define HPLC.
AU8: Please expand CG-MS.
AU9: Please define IFN.
AU10: Please check the following rewritten sentence. '' ANOVA followed by Tukey's post hoc test was used when comparing was made between different groups or a one-way ANOVA followed by Dunnett's post hoc test when comparing was made every mean to a control mean.''
AU11: Please expand TNF-α.
AU12: Ref. 6 was a duplicate entry of ref. 5. So it was deleted and references had been renumbered in the text and in the list to maintain sequential order of citation. Please check.
AU13: Please define HPLC.
AU14: Please expand IFN.
AU15: Please define IFN-β.